A PHYSICAL MECHANISM FOR THE GENERATION OF EXTENDED STELLAR ATMOSPHERES*

by

R. W. Hillendahl†

Department of Astronomy
University of California at Berkeley

and

Lockheed Palo Alto Research Laboratory
3251 Hanover Street
Palo Alto, California

ABSTRACT

A physical mechanism that can result in the generation of extended expanding atmospheres is discussed. The process involves the unloading of stellar material following the arrival of a shock wave at the edge of the star. The basic principles are developed from a discussion of a simplified case that has been studied in the laboratory; they are then applied to the atmosphere of a star. A radiation-hydrodynamics computation of a model cepheid is then used to obtain quantitative atmospheric profiles. The computed continuum and spectral lines during the unloading process are then examined. A discussion of the possibility that the unloading process occurs in stars other than cepheids suggests the existence of a shock visibility factor associated with ionization or dissociation in the region behind the shock front and leads to a possible alternate interpretation of the variable star instability strips in the H-R diagram.

Key words: extended atmospheres, shock waves, hydrodynamics, cepheids.

---

*This work was made possible by a grant of computer time made available by the Berkeley Astronomy Department and by a Lockheed Independent Research Grant.

†Now at Lockheed Palo Alto Research Laboratory, 3251 Hanover Street, Palo Alto, California 93404.

INTRODUCTION

Many stars in the upper part of the Hertzsprung-Russell Diagram appear to have extended atmospheres in which an outwardly directed flow of matter is observed. While a number of probable physical causes of this phenomenon have been studied (cf. Weymann[1]), it is clear that our present understanding is far from satisfactory. In the course of a recent study[2] of atmospheric phenomena in classical cepheids, a mechanism was encountered that can cause atmospheric characteristics similar in many respects to those ascribed to some types of these "steady-state extended atmospheres."

It is the purpose of this presentation to discuss the basic concepts associated with this extension mechanism as studied both theoretically and in the laboratory, and then to apply these concepts to stellar atmospheres. Specific results are then given for a model classical cepheid. Finally, it is suggested that the mechanism may not be confined to cepheid atmospheres, but may be of more general applicability. Some of the consequences of this suggestion are then explored.

THE BASIC PHENOMENA

The phenomena to be discussed are associated with the processes that occur when a shock wave progressing through a gaseous medium arrives at an interface between the material and a vacuum. Previous theoretical studies of these phenomena (cf. Bird[3], Sakurai[4]) as they apply to stars have either employed simplifying assumptions or have failed to establish the relationship between the theoretical results and the associated observable characteristics. Recently however, Zel'dovich and Raizer[5] have reviewed both theoretical and laboratory studies of a much simpler configuration, which provide us with a clearer understanding of the dominant processes that occur.

Their studies concern the emergence of a plane-parallel shock front from a solid, for the case in which the strength of the shock wave is sufficient to cause a conversion of the solid into a gaseous state as the shock front advances through the material. As the shock front arrives in the surface layer, the momentum associated with the shock wave causes the surface layer to "blow-off" into the

https://doi.org/10.1017/S0252921100151334 Published online by Cambridge University Press

vacuum. The rapid expansion of this layer of material lowers the pressure in the surface layer and gives rise to an outwardly directed pressure gradient between the surface layer and the next interior layer of material. This newly created pressure gradient then causes the outflow of additional material. This "unloading" process continues into the deeper layers in the form of a rarefaction wave progressing backward into the material, while the unloaded matter itself is accelerated outward in the direction of the initial motion of the shock wave.

The unloading (rarefaction) wave travels backward into the material with the speed of sound that corresponds to the thermodynamic state behind the shock front. Its velocity is directed opposite to and is smaller in magnitude than that of the shock front. If the original extent of material is large, the unloading process can continue for an extended period of time. The duration of this process can therefore be much greater than the time interval associated with the passage of the shock front through the photosphere. Under suitable circumstances, it can resemble a steady state process.

The unloaded material flows outward with a relatively large velocity which is the result of the outward acceleration experienced by the matter in crossing the shock wave and the additional outward acceleration caused by the pressure gradient in the rarefaction wave. The terminal velocity of a given particle after it unloads to (essentially) zero pressure can be calculated by noting that its terminal kinetic energy is equal to the sum of its kinetic and thermal energy prior to its engulfment by the rarefaction wave. For the simplified case of a nearly weak shock emerging from a material having no pressure gradient prior to arrival of the shock, Zel'dovich and Razier[3] obtain the "velocity doubling law," i.e., the terminal velocity of an unloaded particle is twice the velocity imparted to it by acceleration in the shock front. This result is indicative of the importance of the acceleration in the rarefaction wave, but it apparently represents only a special case. The equations for the general case do not limit the velocity increase to a factor of two, and suggest in fact that much larger increases in velocity may occur if ionization or dissociation is occurring within the rarefaction wave.

The passage of the shock front sets the entire mass of material into motion in the direction in which the shock travels. Thus, while the rarefaction

https://doi.org/10.1017/S0252921100151334 Published online by Cambridge University Press

wave moves "inward" in terms of the mass of the material, it and all parts of the material move "outward" with respect to the laboratory frame of reference.

APPLICATION TO STELLAR ATMOSPHERES

While the situation is much more complicated at the edge of a star due to the presence of the pre-existing motion and/or pressure gradients, the basic physical laws that apply to the laboratory situation should still be operative. Thus, when a shock front arrives at the surface of the star, the unloading of stellar material is to be anticipated. It is further to be expected that the unloading process lasts longer and has therefore a higher probability of observation than the passage of the shock through the photospheric layer. This follows because the unloading process involves the motion of a sonic disturbance into an essentially infinite supply of material, while the shock emergence involves the motion of a supersonic disturbance through a relatively narrow photospheric layer.

Neither the outward flow of the unloaded material nor the inward progress of the rarefaction wave can continue indefinitely in a star. The outward moving particles are accelerated to a finite terminal velocity and are subject to the star's gravitational field. Should the terminal velocity exceed the escape velocity, continued outward motion and mass loss could occur. Particles achieving a lesser than escape velocity will reach a maximum altitude and then be accelerated downward. Differential motion should then occur, which under favorable circumstances, might be observable in terms of the shifting and/or asymmetrical contours of spectral lines. Were the material returning under gravitational acceleration to collide with unloading material still in the process of moving outward, a temperature inversion could occur which would result in emission lines.

An interesting phenomenon can also occur in the rarefaction wave as it moves inward in terms of the mass of the star. As has been noted above, the terminal velocity achieved by a given particle in the unloading process is the sum of the velocity achieved due to passage through the shock front and the velocity achieved due to acceleration in the pressure gradient of the rarefaction wave. This

https://doi.org/10.1017/S0252921100151334 Published online by Cambridge University Press

latter acceleration depends primarily upon the thermal energy of the particle prior to the arrival of the rarefaction wave. As this wave progresses deeper into the mass of the star, the temperature and hence the thermal energy increases. Particles in the deeper layers will thus undergo a greater outward acceleration than the particles in layers initially at larger radii. If these particles from successively deeper layers overtake the particles already unloaded, conditions may be favorable for the formation of a secondary shock wave. When the head of the rarefaction wave passes through a region where ionization or dissociation is occurring, a very rapid increase in particle velocity takes place. Conditions for the formation of a secondary shock are therefore most favorable in such regions of the star.

Such a secondary or "blow-off" shock wave would then progress outward through the star in a manner similar to the original shock wave; the blow-off shock should itself be followed by an inward rarefaction wave similar to that which follows the original shock. Thus a shock wave emerging from a stellar atmosphere should be followed by a series of additional shock waves, reasonably well separated in time, until the process becomes the victim of a damping mechanism or is interrupted by the gravitational return of previously unloaded material.

These secondary shock waves provide a possible explanation[2] for multiple and irregular periods that are well known in variable stars (cf. Arp[6], Abt[7]). The frequency with which the secondary shocks might be anticipated would appear to depend upon the instantaneous atmospheric structure of the star, which in turn must ultimately depend upon the structure of the deep interior. However, it is not clear that there exists any direct connection between the interior structure and the periodicity of the secondary shocks, such as, for example, the relationship that defines the fundamental periodicity of a cepheid. Thus, at the present state of our understanding, one cannot assume that the secondary shocks are strictly periodic or that their period is related to the fundamental period of the star.

It should also be noted that the secondary shocks need not be associated with a pulsating star, but may occur in a localized region of any star so long as the diameter of the region from which a shock wave emerges is large compared to the scale height of the atmosphere. For example, the multiple outward waves seen in certain solar disturbances[8] may be related to the secondary shock process, however, it

is not clear in this instance whether or not the magnetic field merely contributes to or actually causes the observed effect.

If spectral absorption lines originate in layers of a star where unloading of material is occurring, the spectroscopic gravity deduced from the analysis of these lines may be significantly lower than the dynamic gravity derived from the mass and radius of the star. This effect results from the lower pressure gradient that occurs everywhere in a rarefaction wave except in the immediate vicinity of the leading edge of the wave, where the pressure gradient is very steep. The unloading process may therefore offer a possible explanation for the low values of spectroscopic gravity associated with stars of the higher luminosity classes. This mechanism can far outweigh the effects of radiation pressure.

THE CLASSICAL CEPHEID AS AN EXAMPLE

The phenomena discussed above are all governed by a well-defined set of physical equations and can therefore be studied in detail. The relevant equations are the familiar equations of stellar structure, but without the restrictive assumption of hydrostatic equilibrium normally used in stellar evolution computations. As is the case for static stellar structure, analytic solutions are made possible by simplifying assumptions, particularly with regard to the equation of state and the opacity. One can deduce general properties from such solutions, but it is difficult to obtain quantitative models for comparison with observation. One therefore resorts to numerical methods, thereby allowing the inclusion of virtually any desired amount of detail in expressing the thermodynamic and optical properties of the gas.

For the present application, a radiation-hydrodynamics code[9,10] written especially for cepheid computations was employed[2]. The code is a one-dimensional, spherical, lagrangian, LTE, transport code employing an augmented[9] gray absorption coefficient. Convection and stellar rotation are not taken into account. The methods used are a generalization of and are patterned directly after the methods of Henyey, et al.[11]

The final results are independent of the choice of the initial configuration so long as the computations are carried far enough in time so as to be-

https://doi.org/10.1017/S0252921100151334 Published online by Cambridge University Press

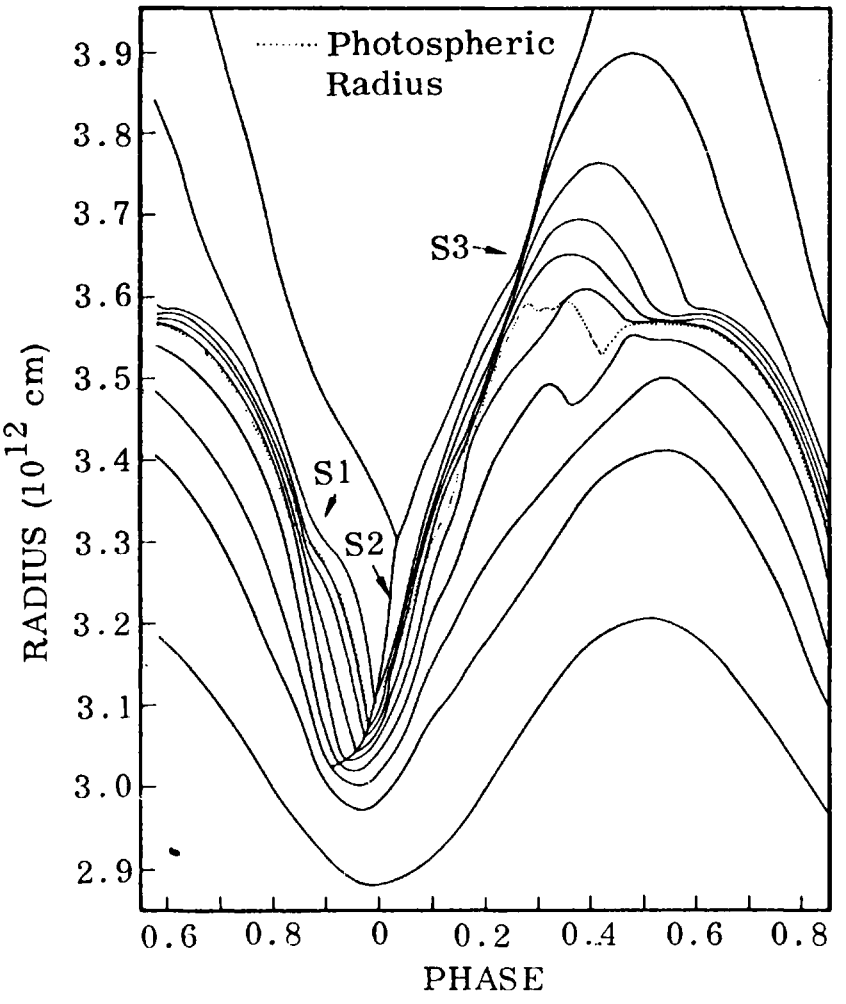

Figure 1. Radius vs time history in the atmosphere layers of a model cepheid.

come reasonably repetitive. The cepheid is therefore an ideal choice for exploratory computations both because the model is relatively free from arbitrary assumptions and because the wealth of available observational data permits a detailed verification of the results. The initial configuration used in present computations consisted of an augmented[2] version of a 7.6-day cepheid model supplied by Christy[12].

In the present context we are interested in the dynamic and optical properties primarily during those phases of the pulsation when unloading occurs. However, for purposes of orientation, Fig. 1 shows the radius versus time history over the entire cycle for every fifth mass point in the computed results. The dotted line represents the photospheric radius. S1 indicates the location of a shock originating in the hydrogen ionization zone which travels inward in terms of radius, but outward in terms of the mass

https://doi.org/10.1017/S0252921100151334 Published online by Cambridge University Press

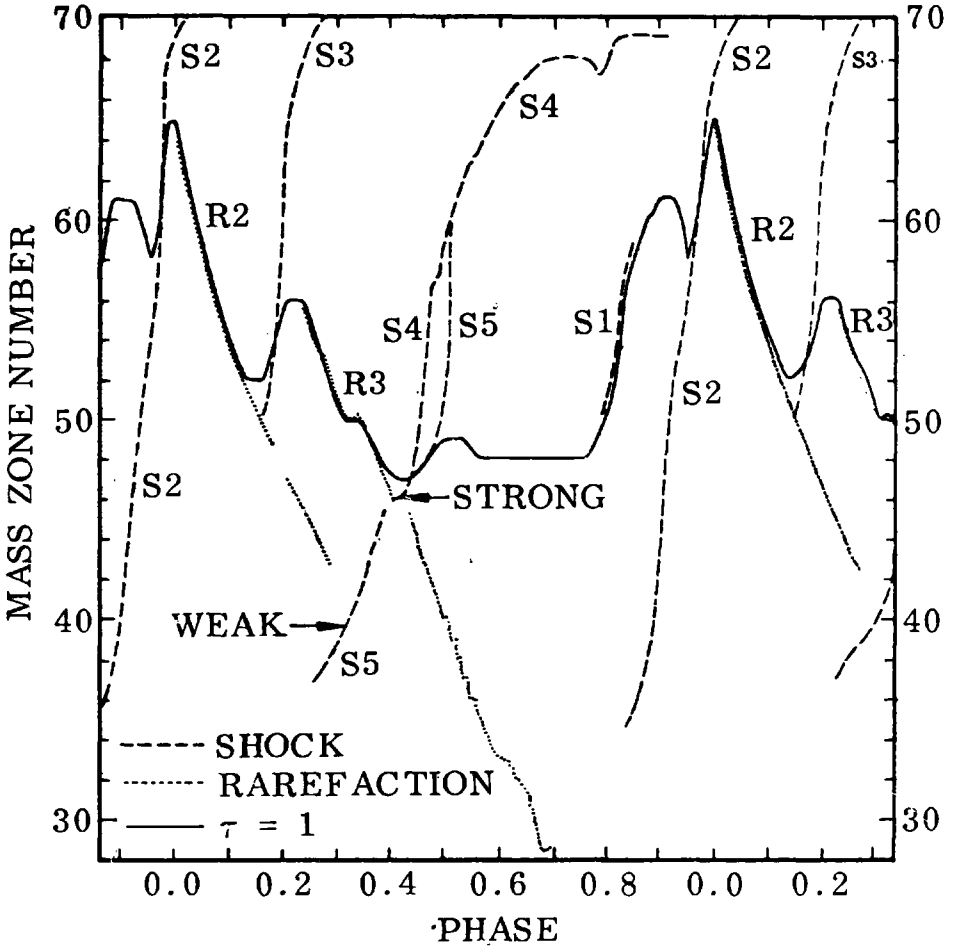

Figure 2. Atmospheric phenomena in a model cepheid.

of the star. This shock causes the bump in the light output during the rise to maximum light, but it is not important to the unloading process. S2 is the primary shock originating in the He II ionization zone which is responsible for the pulsation of the star. It reaches the edge of the star just after maximum light and initiates the unloading process which lasts until a blow-off shock occurs at about phase 0.2.

These events are shown more clearly in Fig. 2 in which the solid line shows the motion of the photosphere throughout the cycle. The short time required for the principal shock S2 to traverse the photosphere, compared to the rarefaction-unloading phase R2, is clearly evident. The process repeats itself as the first blow-off shock S3 traverses the photosphere near phase 0.2 and the resultant rarefaction R3 follows. At about phase 0.35, a bump in the rarefaction R3 can be seen in Fig. 2. This can be identified in Fig. 1 with the reversal of direction

https://doi.org/10.1017/S0252921100151334 Published online by Cambridge University Press

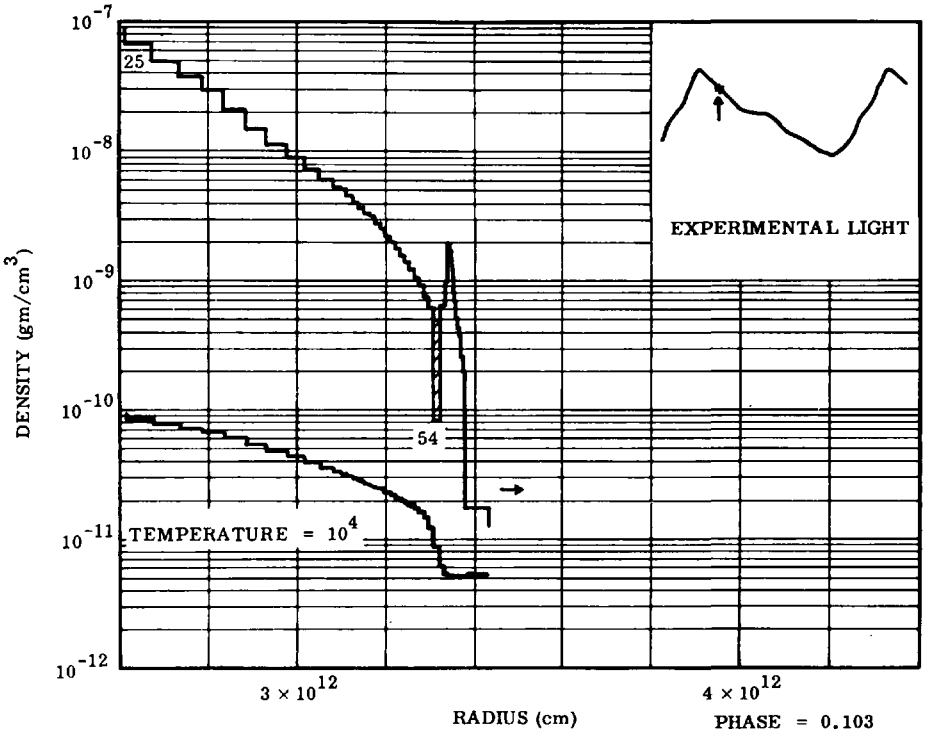

Figure 3. Atmospheric density and temperature profiles during the unloading process.

of the photospheric layers as they reach maximum altitude, and corresponds to the observed secondary maximum in the light output. A second blow-off shock, S4, occurs at phase 0.4, which is soon joined by a reflection S5 of the primary shock off the center of the star. Following this, the atmosphere is characterized by a gravitational collapse. The properties of the model during the rarefaction phase R2 are of primary interest. Fig. 3 shows representative density and temperature profiles during this process. The shaded area serves to locate the photosphere, which occurs at mass zone 54 at this phase. The strange looking density spike is not a shock wave, but is a result of the rarefaction process. As the shock approached the edge of the atmosphere, the rarefaction process had already been initiated in the region behind the shock front. This causes the outward acceleration of material which then overtakes material at larger radii causing a density build-up. The net result is an extended transparent region of relatively high density. The corresponding temperature profile, which has been superposed below the density profile in Fig. 3, shows an extremely steep gradient in the photospheric region, and an extended temperature plateau in the outer atmosphere. The geometrical thickness of this region is approximately

https://doi.org/10.1017/S0252921100151334 Published online by Cambridge University Press

one solar radius at this phase, but becomes almost a factor of 10 larger during the pulsation cycle.

The type of atmospheric profile shown in Fig. 3 results in the emission of a continuum and spectral lines which are different from those which are observed for a hydrostatic atmosphere. Oke[13] has published detailed spectral scanner measurements of the continuum at the appropriate phase (0.1) for the 7.2 day cepheid Eta Aquilae. Six color measurements have also been published by Stebbins, Kron, and Smith[14]. Attempts to match these observations by hydrostatic model atmosphere continua[13,15] have shown that such models cannot be made to fit accurately at both the red and violet extremes of the spectrum.

Using the method of dynamic atmospheres, the author[2] was able to obtain improved correspondence with the observed continuum. This method utilizes a model consisting of a black body source screened by a semi-transparent layer having a given density, temperature, and thickness. The dynamic model fitted to the observations at phase 0.1 consisted of an 8400°K black body screened by a layer of density 10^{-9} gm cm^{-3}, temperature 5500°K, and thickness 1.25×10^{11} cm. The detailed composition of the layer is given in Table 1. The profiles in Fig. 3, from the photospheric layer (zone 54) outward show a close resemblance to this model.

As compared with a hydrostatic atmosphere, the unloading atmosphere has a lower flux in the ultraviolet but has an excess spectral flux near 10,000 A. The extended layer has maximum opacity in the UV and most of the observed radiation is emitted in this layer, while at 10,000 Å the layer is more transparent and most of the radiation originates in the higher temperature photospheric region. The actual spectral continuum computed from the atmospheric profiles given in Fig. 3 agrees qualitatively with the observations, and can be made to agree quantitatively if the temperature in the plateau region is raised about 250°K. The continuum is especially sensitive to this temperature as it determines the population of the Balmer ground state upon which the spectral absorption coefficient is critically dependent.

The absorption lines formed in the atmosphere during the unloading process also show properties that are of interest. Both the unusual temperature and density profiles and the differential motion within the plateau region influence the character of the lines. For a velocity distribution that can be represented analytically, Underhill[16] has demon-

TABLE 1.

DETAILED COMPOSITION AND THERMODYNAMIC PROPERTIES OF DYNAMIC MODEL LAYER FOR ETA AQUILAE AT PHASE 0.1

Total Number Density	4.30×10^{14} /cm^3
Electron Density	3.80×10^{11} /cm^3
HI	3.77×10^{14} /cm^3
HII	3.39×10^{11} /cm^3
H^-	1.76×10^{5} /cm^3
H_2^+	2.44×10^{5} /cm^3
H_2	9.28×10^{8} /cm^3
HeI	5.28×10^{13} /cm^3
HeII	1.63×10^{1} /cm^3
HeIII	———
Metals Composition	GMA
Metals to Hydrogen Ratio	2.0×10^{-3}
Helium to Hydrogen Ratio	0.167
Temperature	5500 °K
Total Pressure	3.289×10^{2} dynes/cm^2
Radiation Pressure	2.3 dynes/cm^2
Gas Pressure	3.266×10^{2} dynes/cm^3
Electron Pressure	0.289 dynes/cm^3
Molecular Weight	1.404 gm/mol
Density	10^{-9} gm/cm^3

strated that a uniformly expanding atmosphere causes the spectral lines to become shallower and broader.

For the present application, a general program was written to accept an arbitrary velocity distribution in the atmosphere. Specific results for selected spectral lines are discussed below. The primary purpose of these calculations is to show the manner in which the dynamic properties of the atmosphere influence the shapes of the spectral lines. No attempt has been made to determine the extent to which these lines agree quantatively with observation.

https://doi.org/10.1017/S0252921100151334 Published online by Cambridge University Press

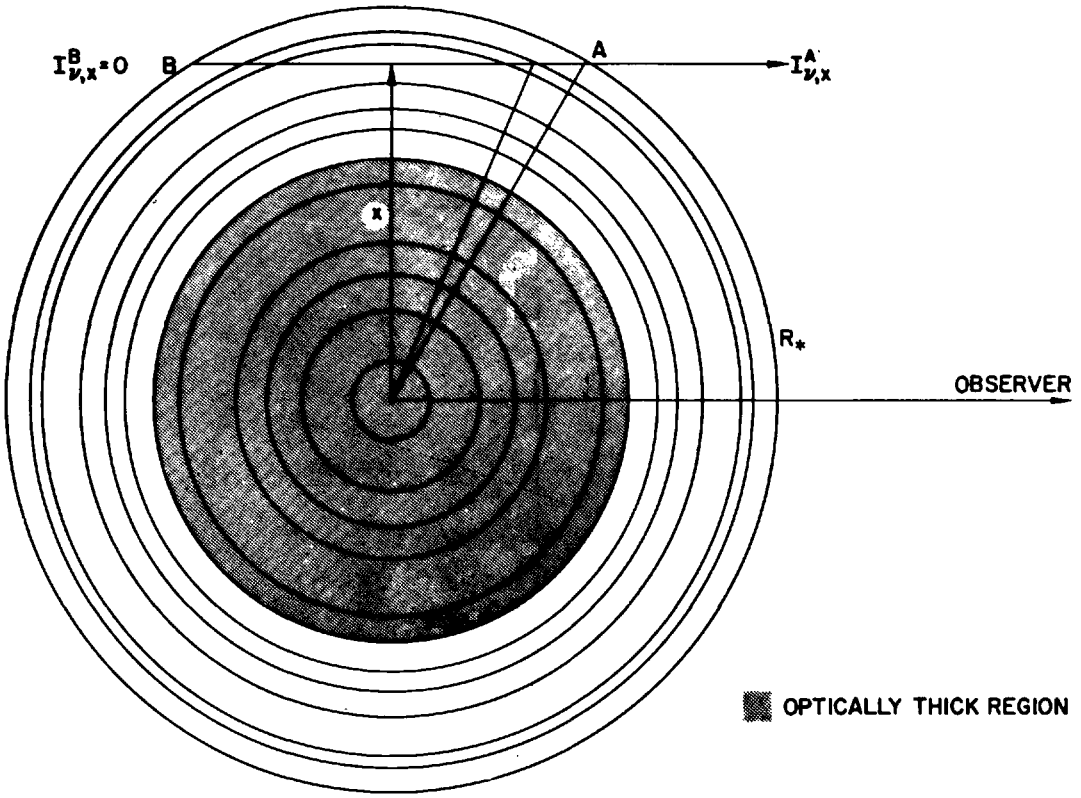

Figure 4. Geometry used in line profile calculations.

Figure 4 shows schematically the instantaneously fixed geometry of a model star consisting of spherical shells of material (70 in the model used here) whose radii, temperatures, densities, and velocities are known from the radiation - hydrodynamics computation. Assuming LTE and a GMA chemical composition, the thermodynamic properties of each shell, including the concentrations of all species, follow from the equation-of-state. The continuum[2] and line absorption[17] coefficients can then be computed directly from the atomic and molecular properties. The Voigt function was evaluated using a routine due to Rybicki[18] while Stark broadening was evaluated using the method of Edmonds, Schulter, and Wells[19].

To obtain the emergent intensity $I^A_{\nu,x}$ for a given radiation frequency, an integration is carried out along a ray path through the star defined by the impact parameter x. Values of x are selected so as to cause the path of integration to bisect each spherical shell as indicated in Fig. 4. The observed flux is then given by

$$F_\nu = 2\,\pi \int_0^{R_*} I^A_{\nu,x}\; x\,dx$$

https://doi.org/10.1017/S0252921100151334 Published online by Cambridge University Press

while the emergent intensity is given by

$$I^{A}_{\nu,x} = \int_{A}^{B} B_{\nu}(\mu\ z)\ e^{-\mu\ z}\ d(\mu\ z)$$

where $\mu = \mu_1 + \mu_c$

μ_c = continuum absorption coefficent

μ_1 = line absorption coefficient

z = geometrical distance measured along the ray path

B_ν = Planck function.

Since the model results from a radiation-hydrodynamics computation, one is not free to choose the zoning structure so as to maintain a small optical thickness for all of the individual shells of material. The source function is therefore interpolated in optical space[9] to achieve greater accuracy. The radial motion of each shell is reduced to a velocity along the ray path in the evaluation of the line absorption coefficient.

The λ 4508 Å line of Fe II was used as a test line to study the effects of the atmospheric motion upon the line shape. Two computed profiles for this line are shown in Fig. 5. The narrow line with steep sides and flat bottom was produced by arbitrarily setting all of the shell velocities to zero. The broadened line results from the velocity distribution given by the radiation-hydrodynamics computation. It is clear from a comparison of these results that the motion of the atmospheric layers broadens the line and increases its equivalent width. The central flux is increased slightly.

Further numerical experimentation, in which the entire atmosphere was assigned a uniform expansion velocity revealed that both the uniform expansion and the differential expansion make significant

https://doi.org/10.1017/S0252921100151334 Published online by Cambridge University Press

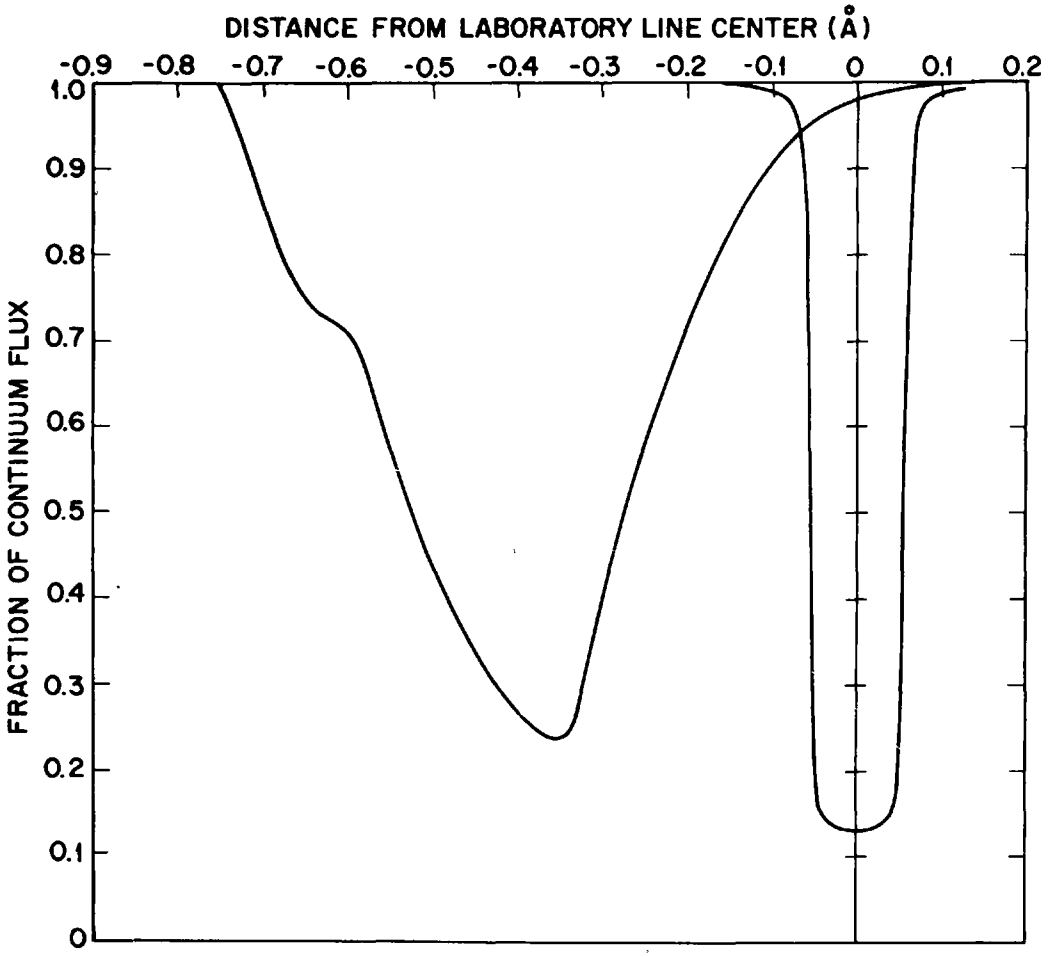

Figure 5. Computed profiles for λ4508Å line of Fe II.

contributions to the line shape. The differential expansion causes an appreciable increase in the equivalent width of the line. The feature on the violet side of the profile is caused by a region of abnormally high outward velocity occurring near the head of the rarefaction wave. The asymmetry of the line appears to be consistent with the analytical results of Van Hoof and Deurinck[20].

The broadened contour of the computed λ 4508 line is similar to the shape for the cepheid SV Vul as observed by Kraft[21], et al. However, in the present computation, neither stellar rotation nor a "turbulent velocity" were assumed in order to produce the line broadening.

The profiles of the first four Balmer lines were also computed. The H_β profile is shown in Fig. 6. The computed profiles for the four lines are all similar, but show a lower central flux and broader wings with increasing principal quantum number. The depression of the continuum over a

https://doi.org/10.1017/S0252921100151334 Published online by Cambridge University Press

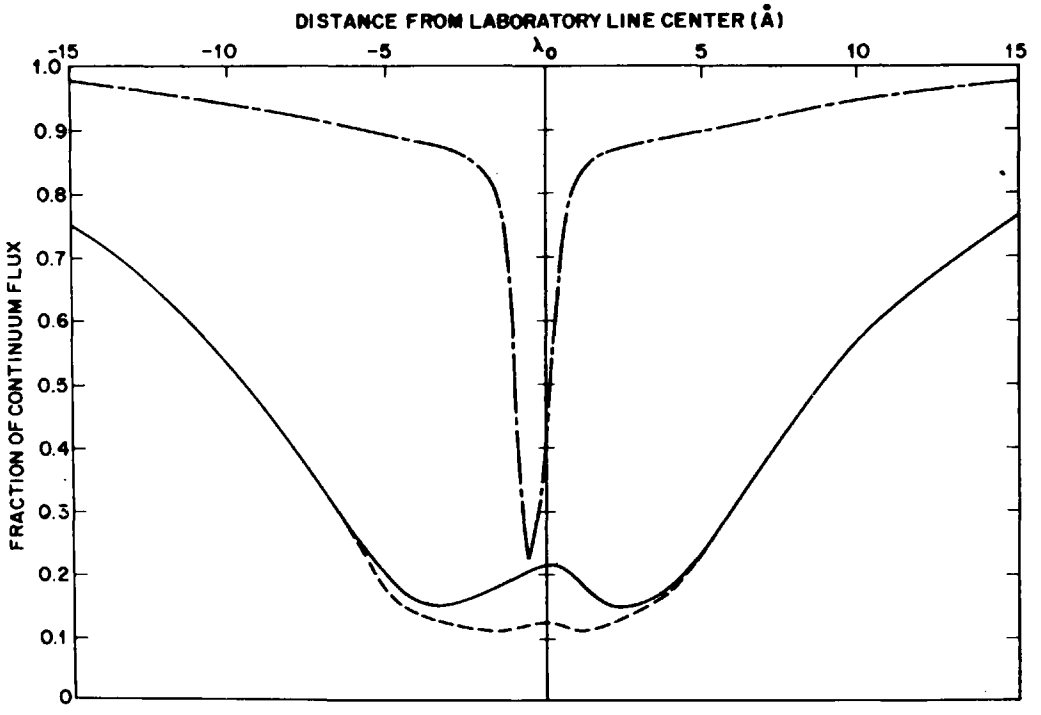

Figure 6. Computed profiles for Hβ and Ca II K lines.

wide region of the spectrum is to be anticipated on the basis of strong wings of these lines. The effect should be particularly evident near the series limit where the wings of the higher members of the Balmer series should overlap and effectively extend the Balmer continuum well to the red of the series limit.

The computed profile for the Ca II K line is also shown in Fig. 6. The line is quite broad and has a weak red shifted emission core. This emission core results from a slight temperature inversion in the outermost shells of the cepheid model as shown in Fig. 3. The dashed line in Fig. 6 shows the change in the K line contour when the outer shell of the cepheid model is arbitrarily removed during the line profile computation. It is interesting to note that the emission core is red shifted, while the absorption profile is blue shifted, even though all parts of the atmosphere are moving outward and might therefore be expected to produce a blue shift. While the reason for this effect has not been positively identified, it apparently is confirmed by the observations of Jacobsen[22].

While the computed profiles have not as yet been quantitatively compared with densitometer profiles, it is clear that the unloading process is capable of producing spectral line characteristics similar to those observed in stars of high luminosity.

https://doi.org/10.1017/S0252921100151334 Published online by Cambridge University Press

GENERALIZATION TO OTHER STARS

A number of lines of evidence indicate the possibility that the unloading mechanism might be operating in stars other than cepheids. Kraft[23], in his extensive discussion of the spectra of supergiants and cepheids, concludes that, "the classical cepheids have spectra that, in detail, are virtually identical with those of the non-variable supergiants at all phases of the variation." Abt[7], in his study of the variability of supergiants, finds that "probably all stars in the H-R diagram above $M_V = +1$ and to the right of the main sequence are variable in light and radial velocity." In addition, he notes that many of the supergiants show a multiple or irregular periodicity in velocity that suggests that secondary shocks might be present.

Taken at face value, these lines of evidence raise the interesting possibility that all luminous stars above the main sequence could actually be variable stars. However, since the stars we normally refer to as "variables" seem to occur in well defined "instability strips" in the H-R diagram, such an interpretation would require that a selection process be operative. Such a selection process could hardly be observational, and would have to have a physical basis.

Historically, the various classes of variable stars have been identified by their relatively large light variations rather than their velocity variations. Abt[7] found that the "non-variable" supergiants have light amplitudes of 0.05 - 0.10 mag., whereas the "variable" stars have light amplitudes on the order of 10 times this amount. The velocities of the "non-variables" have not been studied in sufficient detail to establish any correlation with these light variations. Thus, while it is clear that the existence of instability strips must ultimately be associated with the interior structure of the star, the manner in which this structure manifests itself in terms of observables is not well understood.

A possible cause for the selection phenomenon can be deduced from an analysis of the model cepheid computation discussed earlier. The author[2] found that the large increase in light amplitude in the cepheid resulted from an abrupt spatial density decrease on the back side of the shock front. After shock transparency, this rapid density decrease causes the photosphere to move rapidly inward into

the star, thereby producing a rapid temperature increase in the photospheric region.

It was further found that in the cepheid the steep density decrease behind the shock results from thermal ionization of hydrogen in these layers. If one follows the progress of a given shock from the deep interior of the star to the surface, one finds that the density profile just behind the shock front changes rapidly. Whenever ionization (or dissociation) is occurring behind the shock, a deep density minimum occurs in this region. The density at this minimum may be as low as a factor of 10 below the shock front value. However, when no ionization occurs, the minimum density is rarely more than 30% below the shock front value.

This suggests that the production of a large light amplitude requires that ionization or dissociation occur just behind a shock front during the relatively short time interval when the shock traverses the photosphere. It also implies that the passage of a shock front through the photosphere of a star does not produce large observable effects unless ionization or dissociation is in progress just behind the shock front. This "shock visibility factor" might well be the cause of the apparent instability strips in the H-R diagram.

If one compares the emergence of the primary shock and secondary shocks in the cepheid computation, one finds support for the above interpretation. The shock velocities are nearly equal, but the secondary shocks are followed by only a shallow density minimum. The increase in the computed light output is about 1 mag. for the primary shock emergence, but only about 0.1 mag. for the secondary shock emergence.

There is some observational evidence from variable stars to support this computed result. Bernheimer[24] observed a light increase in Eta Aquilae of 0.15 mag. in 40 minutes. Preston[25] has observed similar rapid low amplitude light variations in RR Lyrae which occur at phases where the emergence of shocks are expected from the radiation-hydrodynamics computations.

A further test of the hypothesis can be made by plotting the traces in the H-R diagram where various ionization and dissociation processes are 50% complete. This can be accomplished by using the data[26] to convert M_V values to log P_e values, and the equation of state. The temperature values associated with these traces are the temperatures in the region behind the shock front. The effective temperature

of the reversing layer just prior to the shock emergence should be lower than this temperature, and systematically related to it. If the major classes of variable stars are superposed on this H-R diagram, it is found that their reversing layer temperatures are about 2/3 of the temperatures where He I ionization, H ionization, and H_2 dissociation are 50% complete. However, this result should be considered as suggestive, rather than conclusive, since the variables occupy rather broad strips in the H-R diagram and it is difficult to establish the M_V - P_e relationship in some parts of the diagram due to the lack of stars. In any event, the unloading process appears to be interesting and should receive further study.

In conclusion, I would like to thank Drs. L. Henyey, R. K. M. Landshoff, R. E. Meyerott, and M. Walt IV for their continued support and encouragement.

REFERENCES

1. R. Weymann, *Astrophys. J.*, 136, 476 (1962).
2. R. W. Hillendahl, Dissertation, Univ. of California at Berkeley (1968).
3. Ya. B. Zeldovich and Yu. P. Raizer, *Physics of Shock Waves and High-Temperature Hydrodynamic Phenomena*, Academic Press, New York and London (1966), pp. 101, 716, 762.
4. G. A. Bird, *Astrophys. J.*, 139, 675 (1964).
5. A. Sakurai, *J. Fluid Mech.*, 1, 436 (1956).
6. H. C. Arp, *Astronomical J.*, 60, 1 (1955).
7. H. A. Abt, *Astrophys. J.*, 126, 138 (1957).
8. G. E. Moreton, *Sky and Telescope*, 21, 145 (1961).
9. R. W. Hillendahl, "Approximation Techniques for Radiation-Hydrodynamics Computations," Defense Atomic Support Agency Report 1522 (1964).
10. R. W. Hillendahl, *Proceedings of the Workshop on the Interdisciplinary Aspects of Radiative Transfer*, ed. R. Goulard Joint Institute for Laboratory Astrophysics, Boulder, Colorado (1965).
11. L. G. Henyey, R. LeLevier, R. D. Levee, K. H. Bohm, and L. Willets, *Astrophys. J.*, 129, 628 (1959).
12. R. H. Christy, California Institute of Technology, private communication (1968).

13. J. B. Oke, *Astrophys. J.*, 133, 90 (1961).
14. J. Stebbins, G. F. Kron, and J. L. Smith, *Astrophys. J.*, 115, 292 (1952).
15. C. Whitney, Dissertation, Harvard University (1955).
16. Anne B. Underhill, *Astrophys. J.*, 106, 128 (1948).
17. L. H. Aller, *Astrophysics*, Ronald Press, New York (1953).
18. G. B. Rybicki, "Routine for Evaluation of the Voigt Function," forwarded by D. G. Hummer.
19. F. N. Edmonds, Jr., F. M. Schluter, and D. C. Wells, III, *Memoirs, Roy. St. Soc.* 71, 271 (1967).
20. A. Van Hoof and R. Deurinck, *Astrophys. J.*, 115, 166 (1952).
21. R. P. Kraft, D. C. Camp, J. D. Fernie, C. Fujita, and W. T. Hughes, *Astrophys. J.*, 129, 50 (1959).
22. T. S. Jacobsen, *Pub. Dominion Ast. Obs. X*, No. 6, 145 (1956).
23. R. P. Kraft, in *Stellar Atmospheres*, ed. J. Greenstein, Univ. of Chicago Press (1960).
24. W. E. Bernheimer, *Lund Medd.*, Ser. II, 61, 11 (1930).
25. G. W. Preston, *Astrophys. J.*, 134, 633 (1961).
26. C. W. Allen, *Astrophysical Quantities*, Univ. of London, Athlone Press (1963), pp. 201, 208.

DISCUSSION

Wellmann: If you extrapolate a nova outburst backward, you will find that a large fraction of the mass has been thrown out during a very short time. This is like the unloading of a shock front. There are also secondary outbursts. Can these be explained by your secondary shock waves? Would your model give the right densities and time scale?

Hillendahl: My model contains many possibilities. It can probably also explain a nova outburst. The production of secondary shock waves by a first shock is a very common physical phenomenon. It is not limited to cepheids, but it is observed in the solar atmosphere as well as in the laboratory; it is also observed with supersonic airplanes and during the re-entry of Gemini space-vehicles.

Lamers: Can your mechanism explain the standing waves in P Cygni type stars, which exist according to a thesis by de Groot?

Hillendahl: Perhaps.

Underhill: It is pleasing to see that your predicted profile for Fe II λ4508 resembles more closely the observed profiles than is the case for outward and inward moving layers. In particular note the difference in asymmetry between the profile from the model with the computed velocity distribution and the profile formed for layers moving with a constant velocity.

Stibbs: I should like to ask, what is the basic physical reason why the proposed shock mechanism leads to a violation of Wesselink's method?

Hillendahl: If you consider the difference between the motion of the masses and the motion of the photospheres you will find a radius that differs by 20 percent from the radius found by Wesselink's method. I think my method is a modified Wesselink-method.

Praderie: Are your results contradictory to Kippenhahn's calculation?

Hillendahl: I didn't say anything about the exciting processes.

Praderie: But how are the shocks produced?

Hillendahl: They are produced by the mechanism given by Christie.

https://doi.org/10.1017/S0252921100151334 Published online by Cambridge University Press